The above discussion for the periodic lens system may be applied directly to the spherical mirror resonator by the relations between mirrors and lenses discussed in Sec. 14.5. A typical optical resonator used in laser systems consists of two spherical mirrors with radii of curvature R_1 and R_2, aligned with a common axis (Fig. 14.6*b*). Rays bounce back and forth between the two mirrors (in the geometrical optics picture), and if the system is stable, they are confined within some maximum radius. From Sec. 14.5, this system is equivalent to the periodic lens systems of Fig. 14.6*a* with $l_1 = l_2 = d$ so that (13) applies directly, with $f_1 = R_1/2$ and $f_2 = R_2/2$. The stability condition for Fig. 14.6*b* is thus

$$0 \leq \left(1 - \frac{d}{R_1}\right)\left(1 - \frac{d}{R_2}\right) \leq 1 \tag{14}$$

It will be shown later that this condition is confirmed by a wave analysis, so it is a very important relation for such resonators. Figure 14.6*c* shows the stable (unshaded) and unstable (shaded) regions in a plane with d/R_1 as ordinate and d/R_2 as abscissa. The special cases shown are the parallel plane ($R_1 = R_2 = \infty$), the concentric ($R_1 = R_2 = d/2$), and the confocal ($R_1/2 + R_2/2 = d$). These will be discussed more in Sec. 14.15 using the wave analysis.

Dielectric Optical Waveguides

14.7 Dielectric Guides of Planar Form

The principle of guiding electromagnetic waves by dielectric guides was shown in Sec. 9.2. Such guides have become very useful for optical communication devices. We will consider the optical fibers used for transmission of optical communication signals in later sections. Here we want to consider the simpler planar forms, which have been utilized in the thin-film devices of integrated optics. Figure 14.7*a* shows such a guide with three dielectrics separated by parallel-plane interfaces. The central medium 2 is often called the *film*, the lower region 3 the *substrate*, and the upper region 1 the *superstrate* or *cover*. If the refractive index of the film is higher than that of the materials above and below, there is the possibility of having guided waves through the phenomenon of total reflection as explained in Sec. 9.2. Here, however, we wish to analyze by returning to the basic field equations.

We assume propagation as $e^{-j\beta z}$ in the z direction of Fig. 14.7*a* and neglect variations with y. In this case the wave solutions divide into TM and TE types. We first consider the latter, with the components E_y, H_x, and H_z. The Helmholtz equation for E_y in each

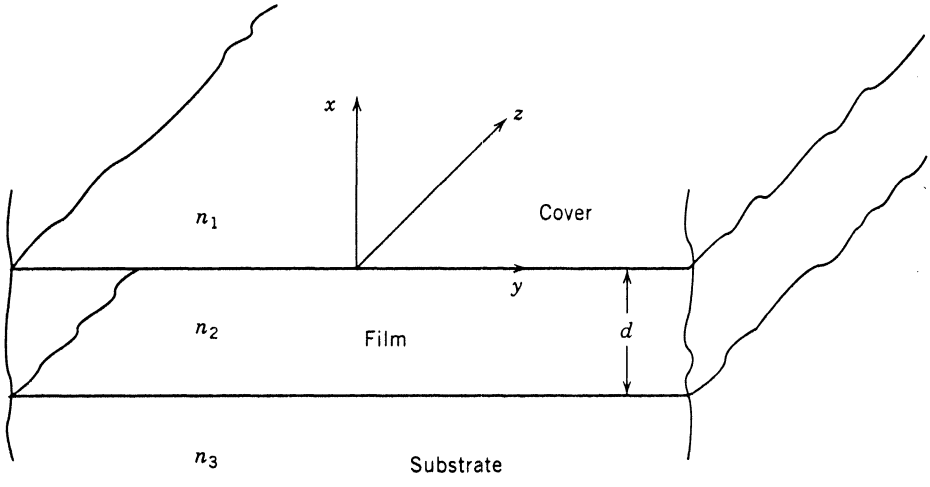

FIG. 14.7a Section of parallel-plane dielectric guide. Propagation is in the z direction.

region is then

$$\frac{d^2E_{yi}}{dx^2} = (\beta^2 - k_i^2)\,E_{yi}, \qquad i = 1,2,3 \tag{1}$$

Solutions of this are either exponentials or sinusoids. We choose exponentials in regions 1 and 3 so that fields may decay with increasing distance from the film. From continuity conditions, it can be shown (Prob. 14.7a) that the solution in the film must then be of sinusoidal form in x. Components H_x and H_z are found, respectively, from the x and z components of the Maxwell equation

$$\nabla \times \mathbf{E} = -j\omega\mu\mathbf{H} \tag{2}$$

The field components of the TE waves in the three regions are then

$$\left.\begin{aligned} E_{y1} &= Ae^{-qx} = -\left(\frac{\omega\mu}{\beta}\right)H_{x1} \\ H_{z1} &= -\frac{1}{j\omega\mu}\frac{\partial E_y}{\partial x} = \frac{q}{j\omega\mu}Ae^{-qx} \end{aligned}\right\} x > 0 \tag{3}$$

$$\left.\begin{aligned} E_{y2} &= B\cos hx + C\sin hx = -\left(\frac{\omega\mu}{\beta}\right)H_{x2} \\ H_{z2} &= \frac{h}{j\omega\mu}\,[B\sin hx - C\cos hx] \end{aligned}\right\} -d \le x \le 0 \tag{4}$$

$$\left.\begin{aligned} E_{y3} &= De^{px} = -\left(\frac{\omega\mu}{\beta}\right)H_{x3} \\ H_{z3} &= -\frac{p}{j\omega\mu}De^{px} \end{aligned}\right\} x < -d \tag{5}$$

where

$$q^2 = \beta^2 - k_1^2, \qquad h^2 = k_2^2 - \beta^2, \qquad p^2 = \beta^2 - k_3^2 \tag{6}$$

Continuity of tangential field components requires that E_y and H_z be continuous at $x = 0$, and again at $x = -d$. The four resulting equations allow reduction from the four arbitrary constants A, B, C, and D to a single one and development of the determinantal equation

$$\tan hd = \frac{h(q + p)}{h^2 - pq} \tag{7}$$

Although this can be solved graphically[9] for the symmetric case and for the useful case in which $n_3 - n_1 \gg n_2 - n_3$ (Prob. 14.7e), it has been solved numerically[10] and the important results are shown in Fig. 14.7*b* with these definitions:

$$v = \frac{2\pi d}{\lambda_0}\sqrt{n_2^2 - n_3^2} \tag{8}$$

$$b = \frac{n_{\text{eff}}^2 - n_3^2}{n_2^2 - n_3^2} \tag{9}$$

$$a = \frac{n_3^2 - n_1^2}{n_2^2 - n_3^2} \tag{10}$$

where

$$n_{\text{eff}} = \frac{\beta}{k_0} \tag{11}$$

It is seen that the parameter v is proportional to the ratio of thickness to wavelength, but also depends upon the differences in refractive index between guiding region and substrate. Parameter b determines the value of β in terms of an effective refractive index n_{eff}. Note that when $b = 0$, the wave travels with the velocity of light in the substrate material, and when b is unity, it travels with the velocity in the film material. The parameter a describes the degree of asymmetry. For $a = 0$, $n_1 = n_3$, and for $a = \infty$, $n_3 - n_1 \gg n_2 - n_3$. As an example of use of the figure, take a glass film on silica substrate with air above, $n_1 = 1$, $n_2 = 1.55$, $n_3 = 1.50$. Thickness $d = 1.46$ μm and $\lambda_0 = 0.6$ μm. Then $v = 6.0$ from (8) and $a = 8.2$ from (10). From Fig. 14.7*b* we find that two modes, the $m = 0$ and $m = 1$ modes, are guided. Their b values are read as 0.82 and 0.31, respectively. Using (9), this gives $n_{\text{eff}} = 1.541$ and 1.516, respectively. Both have velocities between light velocities of film and substrate, but the higher-order wave is nearer cutoff and so has more energy in the substrate and travels with a velocity near c/n_3. The lower-order mode is further from cutoff, has more of its energy in the film, and so has velocity nearer c/n_2.

[9] *R. E. Collin,* Field Theory of Guided Waves, *2nd ed., IEEE Press, Piscataway, NJ, 1991.*
[10] *H. Kogelnik and V. Ramaswamy,* Appl. Opt. ***13****, 1857 (1974).*

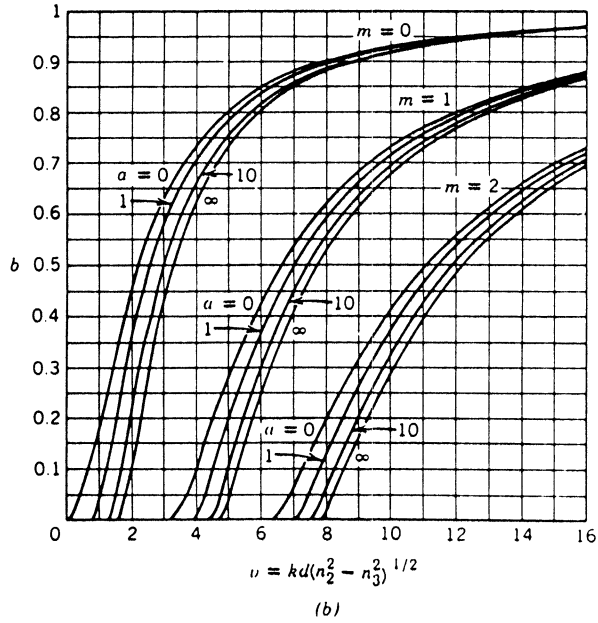

FIG. 14.7*b* Diagram showing normalized phase constant for first few modes of planar slab dielectric waveguides versus normalized frequency, with a range of parameters. (Taken from Kogelnik and Ramaswamy.[10])

For TM waves the analysis is essentially the dual of the above except that we must take into account the different ε's (μ was assumed the same for all regions). The resulting determinantal equation is

$$\tan hd = \frac{h[pn_2^2/n_3^2 + qn_2^2/n_1^2]}{h^2 - pqn_2^4/n_1^2n_3^2} \tag{12}$$

Figure 14.7*b* may also be used for this case when $n_2 \approx n_3$ if a is taken as

$$a_{\text{TM}} = \frac{n_2^4\,(n_3^2 - n_1^2)}{n_1^4\,(n_2^2 - n_3^2)} \tag{13}$$

Note from the figure that for all modes except the $m = 0$ mode for the symmetric case ($n_1 = n_3$), there is a cutoff condition. For lower frequencies or lesser thicknesses, the modes change from guided modes to radiating modes as the condition for total reflection from the interfaces can no longer be satisfied. The ranges are (assuming $n_2 > n_3 > n_1$)

Guided waves	$k_0n_3 < \beta < k_0n_2$
Substrate radiation modes	$k_0n_1 < \beta < k_0n_3$
Modes with radiation above and below	$0 < \beta < k_0n_1$
Physically unrealizable (growing in both regions)	$\beta > k_0n_2$

Although there is only a discrete set of guided modes, there is a continuous spectrum of radiation modes. It can be shown that the modes (including the radiation modes) are orthogonal over the interval $-\infty < x < \infty$ and that the totality of guided and radiation modes form a complete set. However, the set is awkward to use for expansion of arbitrary functions because of the infinite extent of the radiation modes, and their continuous spectrum.[11–13]

Finally we note that although we have developed the determinantal equation from a direct solution of Maxwell's equations, it can also be developed rigorously from the picture of wave reflections at an angle, introduced in Sec. 9.2.

14.8 Dielectric Guides of Rectangular Form

The study of planar guides in the preceding section established the basic principles of dielectric guiding but for most practical purposes it is desirable to confine the wave laterally as well as in depth. One useful configuration is that of a dielectric of rectangular cross section embedded in a substrate of lower index, as indicated in Fig. 14.8*a*. Often the higher dielectric region is formed by diffusion or ion implantation to make an inhomogeneous guiding region, as illustrated in Fig. 14.8*b*. The latter case can be analyzed only numerically once the distribution of index is known (although analytic solutions for certain index variations have been given[13]), but analysis of the rectangular approximation to Fig. 14.8*b* may still be useful. Even the rectangular configuration is hard to analyze, but approximate solutions are available which give a good idea of the behavior.

A numerical analysis of a dielectric guide of rectangular cross section surrounded by a dielectric of lower index was given by Goell.[14] This utilized expansions of the wave in circular harmonics. Most often, one is concerned with operation well above cutoff so that most of the energy is concentrated in the guiding region, and Marcatili has supplied a very useful approximate method for this range.[15] Consider the rectangular dielectric 1 of Fig. 14.8*c*. In the general case, different dielectrics 2, 3, 4, and 5 surround the guiding region. Except near cutoff, the evanescent fields in the external regions die off rapidly so that one need not worry about the difficult problem of matching fields in the shaded corner regions. Moreover, if index differences are not too great, the waves are nearly transverse electromagnetic and are found to break into two classes: E^x_{pq} with

[11] *D. Marcuse,* Light Transmission Optics, *2nd ed., Krieger, Melbourne, FL, 1982.*
[12] *D. Marcuse,* Theory of Dielectric Optical Waveguides, *2nd ed., Academic Press, San Diego, CA, 1991.*
[13] *H. Kogelnik, in* Guided Wave Optoelectronics *(T. Tamir, Ed.), 2nd ed., Springer-Verlag, New York, 1990.*
[14] *J. E. Goell,* Bell. Syst. Tech. J. ***48**, 2133 (1969).*
[15] *E. A. J. Marcatili,* Bell Syst. Tech. J. ***48**, 2071 (1969).*

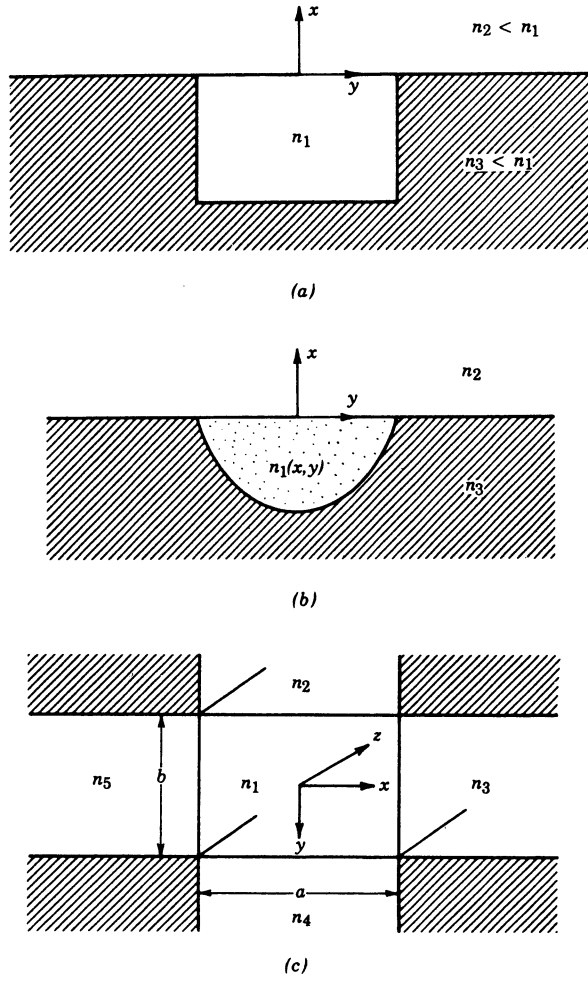

FIG. 14.8 (*a*) Dielectric guide with guiding confined in the *y* direction. (*b*) Similar inhomogeneous guide made by diffusion or ion implantation techniques. (*c*) Model for Marcatili analysis.

negligible E_y, and E_{pq}^y with negligible E_x. For the latter class, with propagation as $e^{-j\beta z}$,

$$E_{y1} = C_1 \cos(k_x x + \phi_1) \cos(k_y y + \phi_2) \tag{1}$$

$$E_{y2} = C_2 \cos(k_x x + \phi_1) e^{\alpha_2 y} \tag{2}$$

$$E_{y3} = C_3 e^{-\alpha_3 x} \cos(k_y y + \phi_2) \tag{3}$$

where

$$\alpha_2 = [\beta^2 + k_x^2 - k_2^2]^{1/2} \tag{4}$$

$$\alpha_3 = [\beta^2 + k_y^2 - k_3^2]^{1/2} \tag{5}$$

The solution for region 4 is similar to that for 2, and the solution for region 5 is similar to that for 3, but with exponentials of opposite sign. Remaining field components are obtained from Maxwell's equations. Components E_x and H_y are negligible for this class; continuity of other tangential components at the four boundaries $x = \pm a/2, y = \pm b/2$ relate all constants to C_1 and give the determinantal equation for β. Figure 14.8*d* gives results when all surrounding dielectrics are the same, $n_5 = n_4 = n_3 = n_2$, with $n_1/1.05$

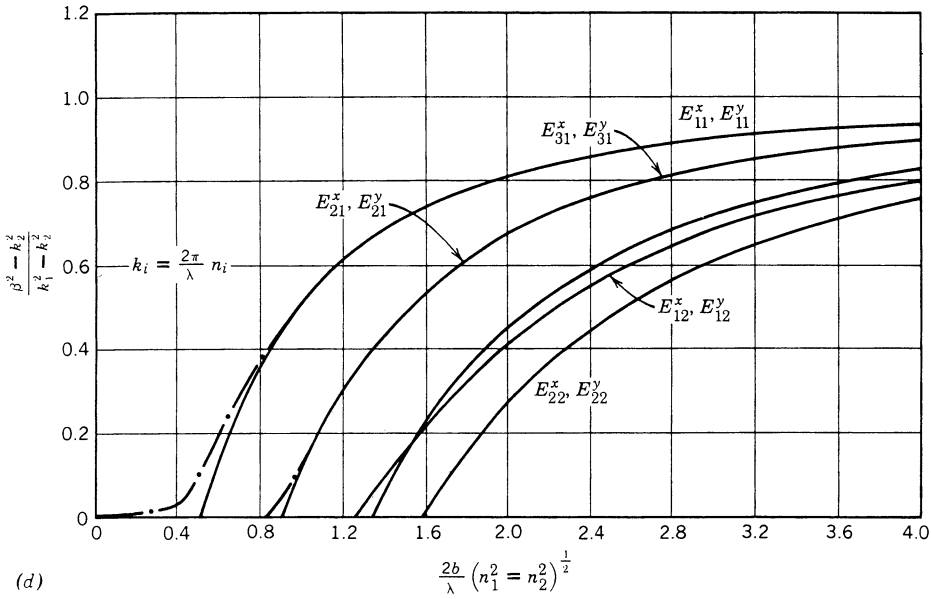

(*d*)

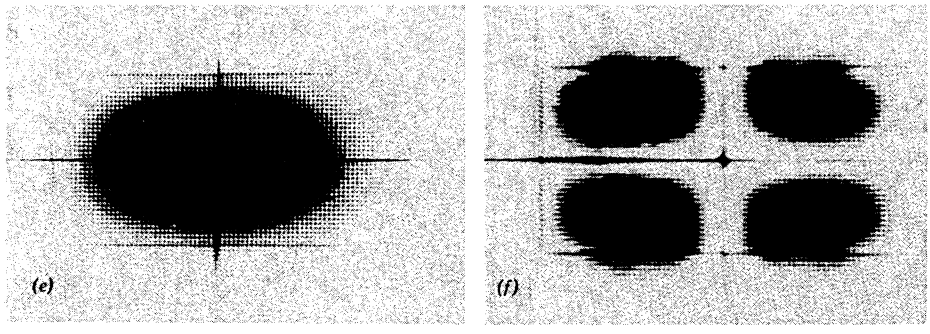

FIG. 14.8 (*d*) Curves giving normalized phase constant versus normalized frequency of several modes in rectangular dielectric guide surrounded by a common dielectric. Solid curves are by Marcatili's approximate method,[15] and dot–dash curves by Goell's computer solutions.[14] (*e*) Intensity picture of E_{11}^y mode for $a/b = 2$ from Goell.[14] (*f*) Similar picture for E_{22}^y mode.[14] Figs. *d*, *e*, and *f* reprinted with permission of the *Bell System Technical Journal*, Copyright 1969, AT&T.

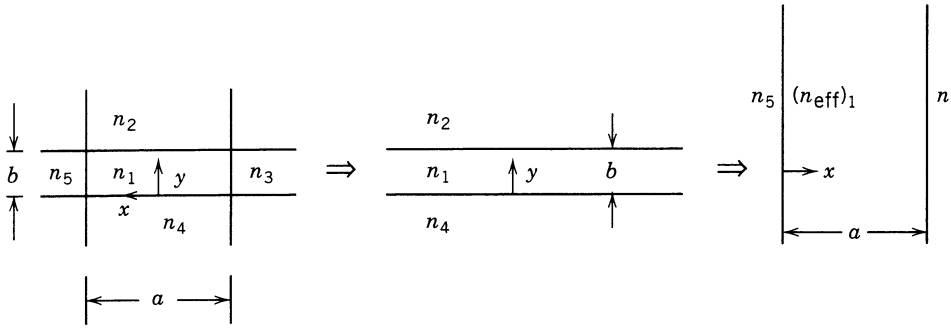

FIG. 14.8*g* Two-step method for obtaining effective index for a rectangular dielectric guide.

$< n_2 < n_1$ and $b/a = \frac{1}{2}$. Also plotted for comparison are results from Goell's computer calculations for these parameters showing that there is good agreement except near cutoff. Figures 14.8*e* and *f* show a picture of two E^y_{mn} modes in a dielectric with $b/a = \frac{1}{2}$, $n_1 = 1.02$, $n_2 = 1$, and $(2b/\lambda_0)(n_1^2 - n_2^2)^{1/2} = 2$.

Effective Index Method Many important guiding systems used with semiconductor lasers or integrated optics have lateral dimensions of the guiding regions appreciably larger than the depths. That is, $a \gg b$ in Fig. 14.8*c*. In such cases a simple method called the *effective index method* has been used to give useful approximate results.[16] The basis for this approach is in the recognition that for such cases the variations in the vertical direction are dominant, assuming comparable mode orders in x and y. Thus, in the Helmholtz equation with the $e^{-j\beta z}$ propagation factor,

$$\frac{\partial^2 E}{\partial x^2} + \frac{\partial^2 E}{\partial y^2} = (\beta^2 - k^2)E \tag{6}$$

the second derivative in x can be neglected in the first approximation. The solution is then that of the planar guide of Sec. 14.7, with y as the variable instead of x. The curves of Fig. 14.7*b* may then be used to give a first approximation to effective index, $(n_{eff})_1$. Confinement in the x direction is then accounted for by using this effective index between the side dielectrics, n_3 and n_5, and again using the planar analysis of Fig. 14.7*b* with only x variations, leading to an improved $n_{eff} = \beta/k_0$. The two steps are indicated in Fig. 14.8*g*.

As with the Marcatili method, the effect of the corner materials is omitted, and as with that method, results are best when operation is well above cutoff.

[16] *J. Bous,* IEEE J. Quant. Electronics **QE-18**, *1083 (1982).*

14.9 Dielectric Guides of Circular Cross Section

Many practical dielectric guides, including the fibers used for optical communications, are of circular cross section. We consider in this section a dielectric with uniform permittivity ε_1 extending to $r = a$, with a second dielectric of lower permittivity ε_2 surrounding it, and permeability of both materials taken as μ_0 (Fig. 14.9*a*). (This is called a *step index fiber* in optical communications; the useful *graded index fiber* is discussed in the next section.)

Any rectangular component of field, such as E_z, satisfies the scalar Helmholtz equation, which for a wave propagating as $e^{\mp j\beta z}$, in circular cylindrical coordinates, is

$$\frac{\partial^2 E_z}{\partial r^2} + \frac{1}{r}\frac{\partial E_z}{\partial r} + \frac{1}{r^2}\frac{\partial^2 E_z}{\partial \phi^2} + (k^2 - \beta^2)E_z = 0$$

For guided modes, $k_1^2 - \beta^2 > 0$ in the core, so ordinary Bessel functions result there. Only the first kind is used, to maintain fields finite on the axis. For the outer material or cladding, $\beta^2 - k_2^2 > 0$ for guided modes so that modified Bessel functions are utilized. Only the second solution is retained, so that fields die off properly at infinity. Axial field H_z satisfies a similar equation and we may write

$$\begin{array}{ll} r < a & r > a \\ E_{z1} = AJ_l\left(\dfrac{ur}{a}\right)\begin{Bmatrix}\cos l\phi \\ \sin l\phi\end{Bmatrix} & E_{z2} = CK_l\left(\dfrac{wr}{a}\right)\begin{Bmatrix}\cos l\phi \\ \sin l\phi\end{Bmatrix} \\ H_{z1} = BJ_l\left(\dfrac{ur}{a}\right)\begin{Bmatrix}\sin l\phi \\ \cos l\phi\end{Bmatrix} & H_{z2} = DK_l\left(\dfrac{wr}{a}\right)\begin{Bmatrix}\sin l\phi \\ \cos l\phi\end{Bmatrix} \\ u^2 = (k_1^2 - \beta^2)a^2 & w^2 = (\beta^2 - k_2^2)a^2 \end{array} \tag{1}$$

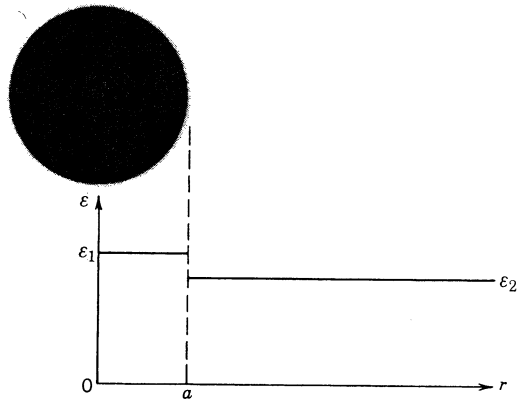

Fig. 14.9*a* Step index optical fiber.

The transverse field components may be obtained from these through Eqs. 8.9(1)–(4), where $k_{c1}^2 = u^2/a^2$ for region 1 and $k_{c2}^2 = -w^2/a^2$ for region 2. The results for E_ϕ and H_ϕ (needed in applying continuity) are

$$E_{\phi 1} = \left[\pm \frac{j\beta a^2 l}{ru^2} AJ_l\left(\frac{ur}{a}\right) + \frac{j\omega\mu a}{u} BJ_l'\left(\frac{ur}{a}\right) \right] \begin{Bmatrix} \sin l\phi \\ \cos l\phi \end{Bmatrix} \tag{2}$$

$$E_{\phi 2} = \left[\mp \frac{j\beta a^2 l}{rw^2} CK_l\left(\frac{wr}{a}\right) - \frac{j\omega\mu a}{w} DK_l'\left(\frac{wr}{a}\right) \right] \begin{Bmatrix} \sin l\phi \\ \cos l\phi \end{Bmatrix} \tag{3}$$

$$H_{\phi 1} = \left[-\frac{j\omega\varepsilon_1 a}{u} AJ_l'\left(\frac{ur}{a}\right) \mp \frac{j\beta a^2 l}{u^2 r} BJ_l\left(\frac{ur}{a}\right) \right] \begin{Bmatrix} \cos l\phi \\ \sin l\phi \end{Bmatrix} \tag{4}$$

$$H_{\phi 2} = \left[\frac{j\omega\varepsilon_2 a}{w} CK_1'\left(\frac{wr}{a}\right) \pm \frac{j\beta a^2 l}{w^2 r} DK_l\left(\frac{wr}{a}\right) \right] \begin{Bmatrix} \cos l\phi \\ \sin l\phi \end{Bmatrix} \tag{5}$$

For the symmetric case with $l = 0$, the solutions break into separate TM and TE sets, the former with E_z, H_ϕ, and E_r (expression for the last component not shown) and the TE set with H_z, E_ϕ, and H_r. The continuity condition of $E_{z1} = E_{z2}$ and $H_{\phi 1} = H_{\phi 2}$ at $r = a$ gives for the TM set

$$\frac{J_1(u)}{J_0(u)} = -\frac{\varepsilon_2 u}{\varepsilon_1 w} \frac{K_1(w)}{K_0(w)} \tag{6}$$

The continuity condition of $H_{z1} = H_{z2}$, $E_{\phi 1} = E_{\phi 2}$ at $r = a$ for the TE set gives the same equation with the factor $\varepsilon_2/\varepsilon_1$ missing. Cutoff for the dielectric guide may be considered to be the condition for which fields in the outer guide extend to infinity, which happens if $w = 0$. For $w = 0$, $K_1/K_0 = \infty$, so that $J_0(u_c) = 0$. So at cutoff,

$$u_c = a(k_1^2 - k_2^2)^{1/2} = 2.405, 5.52, \ldots \tag{7}$$

If $l \neq 0$, the fields do not separate into TM and TE types, but all fields become coupled through the continuity conditions. Applying continuity of E_z, H_ϕ, H_z, and E_ϕ at $r = a$, the four arbitrary constants of (1)–(5) reduce to a single constant and there results the determinantal equation

$$\left[\frac{k_1 J_l'(u)}{uJ_l(u)}\right]^2 + \left[\frac{k_2 K_l'(w)}{wK_l(w)}\right]^2 + \frac{(k_1^2 + k_2^2)}{uw}\left[\frac{J_l'(u)K_l'(w)}{J_l(u)K_l(w)}\right] = \frac{\beta^2 l^2 v^4}{u^4 w^4} \tag{8}$$

where

$$v = \sqrt{u^2 + w^2} = \frac{2\pi a}{\lambda}\sqrt{n_1^2 - n_2^2} \tag{9}$$

Solutions of this transcendental equation leads to *hybrid modes*. Although not purely TM or TE, H_z is dominant in one set of solutions, designated HE_{lp} modes, whereas E_z is dominant in a set designated EH_{lp} modes. Curves of β/k_0 as a function of v are shown for several of the modes in Fig. 14.9*b*.[17] The HE_{11} mode is special in that it has

[17] *D. B. Keck, in* Fundamentals of Optical Fiber Communications *(M. L. Barnoski, Ed.), Academic Press, San Diego, CA, 1976.*

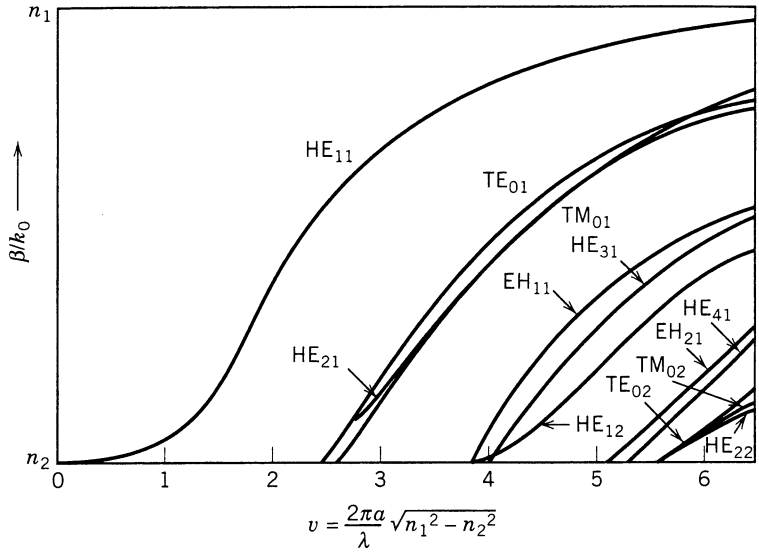

FIG. 14.9b Normalized propagation constant as a function of v parameter for a few of the lowest-order modes of a step waveguide.[17]

no cutoff frequency and so is often called the *dominant mode*. Although it has no strict cutoff, energy is primarily in the guiding core only when the core size is appreciable in comparison with wavelength. This mode has been used in dielectric radiators[18] and is also important in optical fibers.[19] Some photographs of the light distribution in various modes or combinations of modes are shown in Fig. 14.9*c*. For high-data-rate fiber communications it is desirable to have only one propagating mode to avoid intermode distortion, as will be further discussed in Sec. 14.11.

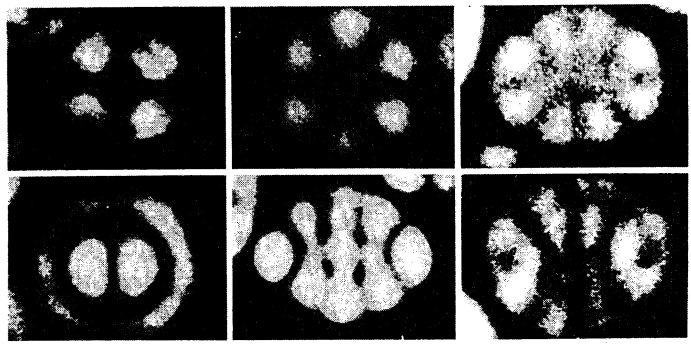

FIG. 14.9c Photographs of modes in the step-index optical fiber. (From Ref. 19.)

[18] *G. E. Mueller and W. A. Tyrrell,* Bell Syst. Tech. J. ***26****, 837 (1947).*
[19] *N. S. Kapany,* J. Opt. Soc. Am. ***51****, 1067 (1961).*

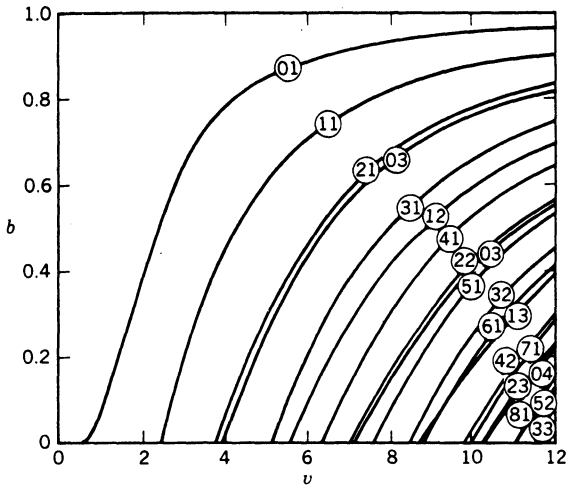

(d)

FIG. 14.9*d* Normalized propagation constant versus normalized frequency for weakly guided modes. (From Gloge.[21])

Special Case of Weak Guiding Most fibers used in optical communications have only a small index difference between the inner core and the outer cladding. It has been shown[20,21] that in this case the determinantal equation (8) greatly simplifies and that modes of order $l + 1$ and $l - 1$ have nearly the same values of β. When these nearly degenerate modes are superposed, it is found that fields combine in such a way that they are linearly polarized—one set with E_x and H_y and another with E_y and H_x as the dominant fields. Thus a wave with E_x constructed from the $l + 1, p$ and $l - 1, p$ hybrid modes is designated $LP^x_{l,p}$. Curves of phase constant (normalized) for these "weakly guided" modes have been calculated by Gloge[21] and are shown in Fig. 14.9*d*. The variable v is given by (9); b is similar to that used with planar guides and is defined as

$$b = \frac{[\beta^2/k_0^2 - n_2^2]}{[n_1^2 - n_2^2]} = \frac{[\beta/k_0 - n_2][\beta/k_0 + n_2]}{[n_1 - n_2][n_1 + n_2]} \tag{10}$$

Since n_1, n_2, and β/k_0 are all near one another, the factors with positive sign essentially cancel and

$$b \approx \frac{[\beta/k_0 - n_2]}{[n_1 - n_2]} \tag{11}$$

[20] *A. W. Snyder and J. D. Love,* Optical Waveguide Theory, *Chapman and Hall, London, 1983.*

[21] *D. Gloge,* Appl. Opt. ***10****, 2252 (1971).*

14.10 Propagation of Gaussian Beams in Graded Index Fibers

Dielectric rods or fibers with a quadratic variation of index with radius (or nearly so) are found to be very useful for guiding optical waves. From a ray optics point of view each section appears as a lens, with a consequent confining of rays by this distributed lens as shown in Ex. 14.4b. We now wish to study the guided modes of such a rod by a field analysis and will find that the fundamental mode has a gaussian distribution over the cross section. Later we will see similar gaussian modes in space, but spreading in the absence of a guiding medium. Gaussian modes and their higher-order extensions are consequently of major importance in work with coherent optics and we will find ways of studying their transformation by lenses, mirrors, and other optical components.

Let permeability be that of space with ε a function of radius. Maxwell's equations are

$$\nabla \cdot [\varepsilon(r)\mathbf{E}] = \varepsilon \nabla \cdot \mathbf{E} + \mathbf{E} \cdot \nabla \varepsilon = 0 \tag{1}$$

$$\nabla \times \mathbf{H} = j\omega\varepsilon(r)\mathbf{E} \tag{2}$$

$$\nabla \times \mathbf{E} = -j\omega\mu_0\mathbf{H} \tag{3}$$

As usual, we take the curl of (3):

$$\nabla \times \nabla \times \mathbf{E} = -j\omega\mu_0 \nabla \times \mathbf{H} \tag{4}$$

The left side is expanded and (2) is substituted on the right:

$$-\nabla^2\mathbf{E} + \nabla(\nabla \cdot \mathbf{E}) = \omega^2\mu_0\varepsilon(r)\mathbf{E} \tag{5}$$

Now $\nabla \cdot \mathbf{E}$ is substituted from (1) and the terms rearranged to give

$$\nabla^2\mathbf{E} + \omega^2\mu_0\varepsilon(r)\mathbf{E} = -\nabla\left(\frac{\mathbf{E} \cdot \nabla\varepsilon}{\varepsilon}\right) \tag{6}$$

This is the general equation for $\mathbf{E}$ in a region with inhomogeneous ε. However, if the change of ε is small in a wavelength, as is usual, it can be shown that the term on the right is small in comparison with the second term on the left. We consequently neglect the right side:

$$\nabla^2\mathbf{E} + \omega^2\mu_0\varepsilon(r)\mathbf{E} \approx 0 \tag{7}$$

We take the variation of ε as quadratic in n:

$$\varepsilon(r) = \varepsilon_0 n^2(r) = \varepsilon_0 n^2(0)\left[1 - \Delta\left(\frac{r}{a}\right)^2\right]^2 \tag{8}$$

where $n(r)$ is the corresponding index variation and a is some reference radius. For one transverse rectangular component of $\mathbf{E}$, Eq. (7), neglecting the term in Δ^2, becomes

$$\nabla^2 E + k^2(0)\left[1 - 2\Delta\left(\frac{r}{a}\right)^2\right]E = 0 \tag{9}$$

where

$$k^2(0) = \omega^2\mu_0\varepsilon(0) = \frac{\omega^2}{c^2}n^2(0) = \left(\frac{2\pi}{\lambda_0}\right)^2 n^2(0) \tag{10}$$

Let us first consider circular cylindrical coordinates with no ϕ variations. Equation (9) then becomes

$$\frac{\partial^2 E}{\partial r^2} + \frac{1}{r}\frac{\partial E}{\partial r} + \frac{\partial^2 E}{\partial z^2} + k^2(0)\left[1 - 2\Delta\left(\frac{r}{a}\right)^2\right]E = 0 \tag{11}$$

It can be shown by substitution that this is solved by

$$E(r, z) = Ae^{-(r/w)^2}e^{-j\beta z} \tag{12}$$

where

$$w = \left(\frac{2a^2}{\Delta k^2(0)}\right)^{1/4} = \left[\frac{a\lambda_0}{\pi n(0)}\right]^{1/2}\left(\frac{1}{2\Delta}\right)^{1/4} \tag{13}$$

and

$$\beta = k(0) - \frac{2}{w^2 k(0)} = k(0) - \frac{2}{a}\left(\frac{\Delta}{2}\right)^{1/2} \tag{14}$$

so that the variation of E with radius is of gaussian form with a radius w to the $1/e$ value of field dependent upon a, λ_0, $n(0)$, and Δ. This radius is usually called *beam radius* although fields do extend beyond. As a numerical example, if $\Delta = 0.01$, $a = 50\ \mu$m, $\lambda_0 = 1\ \mu$m, $n(0) = 1.5$, w is found to be 8.67 μm.

When w is large compared with wavelength, transverse variation of E is small in a wavelength, and the mode is nearly transverse electromagnetic with axial components of **E** and **H** negligible and the transverse components normal to each other and related by $[\mu_0/\varepsilon(0)]^{1/2}$. This fundamental mode is consequently designated TEM_{00}.

Higher-order modes may be found by returning to (9). First by expansion of ∇^2 in rectangular coordinates,

$$\frac{\partial^2 E}{\partial x^2} + \frac{\partial^2 E}{\partial y^2} + \frac{\partial^2 E}{\partial z^2} + k^2(0)\left[1 - 2\Delta\left(\frac{r}{a}\right)^2\right]E = 0 \tag{15}$$

the solution may be shown to be

$$E = A_{mp}H_m\left(\frac{\sqrt{2}x}{w}\right)H_p\left(\frac{\sqrt{2}y}{w}\right)e^{-(x^2+y^2)/w^2}e^{-j\beta_{mp}z} \tag{16}$$

where $H_m(\zeta)$ are Hermite polynomials of order m satisfying the differential equation[22]

[22] *M. R. Spiegel,* Mathematical Handbook, *Schaum's Outline Series, McGraw-Hill, New York, 1968.*

$$\frac{d^2H_m(\zeta)}{d\zeta^2} - 2\zeta\frac{dH_m(\zeta)}{d\zeta} + 2mH_m(\zeta) = 0 \tag{17}$$

and defined by

$$H_m(\zeta) = (-1)^m e^{\zeta^2}\frac{d^m}{d\zeta^m}e^{-\zeta^2} \tag{18}$$

In these higher-order modes, w is the same as in (13) but β_{mp} is given by

$$\beta_{mp}^2 = k^2(0) - 2\frac{\sqrt{2\Delta}}{a}k(0)(m + p + 1) \tag{19}$$

Or with Δ small,

$$\beta_{mp} \approx k(0) - \frac{\sqrt{2\Delta}}{a}(m + p + 1) \tag{20}$$

Similarly if ∇^2 is expanded in circular cylindrical coordinates, (9) is

$$\frac{\partial^2 E}{\partial r^2} + \frac{1}{r}\frac{\partial E}{\partial r} + \frac{1}{r^2}\frac{\partial^2 E}{\partial \phi^2} + \frac{\partial^2 E}{\partial z^2} + k^2(0)\left[1 - 2\Delta\left(\frac{r}{a}\right)^2\right]E = 0 \tag{21}$$

The solution may be shown to be

$$E = B_{mp}\left(\frac{\sqrt{2}r}{w}\right)^m L_p^m\left(\frac{2r^2}{w^2}\right)e^{-r^2/w^2}e^{\pm jm\phi}e^{-j\beta_{mp}z} \tag{22}$$

where $L_p^m(\xi)$ are associated Laguerre polynomials[22] of order p and degree m, satisfying the differential equation

$$\xi\frac{d^2L_p^m(\xi)}{d\xi^2} + (m + 1 - \xi)\frac{dL_p^m(\xi)}{d\xi} + (p - m)L_p^m(\xi) = 0 \tag{23}$$

and defined by

$$L_p^m(\xi) = \frac{d^m}{d\xi^m}\left[e^{\xi}\frac{d^p}{d\xi^p}(\xi^p e^{-\xi})\right] \tag{24}$$

Here also w is as in (13) but phase constant β is

$$\beta \approx k(0) - \frac{\sqrt{2\Delta}}{a}(2m + p + 1) \tag{25}$$

Since the fiber is cylindrical, it might seem that we would only be interested in the latter set, but the Hermite forms are not only simpler, but are often generated by asymmetric excitations. Each of the sets is complete, so an arbitrary distribution can be expanded in either of the two sets.

14.11 Intermode Delay and Group Velocity Dispersion

In an information transmission system, the optical wave is modulated (often digitally) and by Fourier analysis there must be a band of frequencies transmitted to represent the modulated wave. If group velocity varies over this frequency band, the envelope is distorted as the signal propagates down the fiber, as shown in Sec. 8.16. Such *group dispersion* limits the useful transmission distance for a given information rate. We shall see below that group dispersion may arise either from material properties or from the characteristics of waveguide modes themselves. In addition, signal distortion may arise in multimode guides because of the different velocities of the various modes, even at the same frequency; this effect will be considered first.

Intermode Delay In a fiber with many propagating modes, Figs. 14.9*b* and *d* show that some modes will be near cutoff with most of the energy in the cladding, some will be far from cutoff with most of the energy in the core, and others will be in between. Thus a single pulse at the input, if it excites multiple modes, may end as a multiple pulse at the output and an estimate of intermode group delay for length L of the multimode fiber is

$$\Delta T_g = \frac{L}{c}(n_1 - n_2) \tag{1}$$

For a 1% difference in n_1 and n_2, with n about 1.5, the initial pulse would yield multiple pulses spread over about 50 ns for each kilometer of propagation, severely limiting for high-data-rate, long-distance systems.

An advantage of the graded index fiber is that intermode delay is less limiting than in the above. If we calculate group velocity from the approximate expression for β of a quadratic index fiber, Eq. 14.10(20), group delay for mode (m, p) is

$$T_g = L\frac{d\beta_{mp}}{d\omega} = \frac{L}{c}\left[n(0) + \frac{\omega dn(0)}{d\omega}\right] \tag{2}$$

Thus, to this degree of approximation, group delay is the same for all modes and we do not receive multiple pulses at the output corresponding to a single pulse at the input. The more accurate expression 14.10(19) would show some intermode delay and practical differences between the real graded fiber and the ideal model also add some delay, but graded index fibers are capable of appreciably higher data rates for a given distance than the step index fibers for which (1) was an estimate.

Group Velocity Dispersion For a single mode, group delay over length L is

$$T_g = \frac{L}{v_g} = L\frac{d\beta}{d\omega} \tag{3}$$

So for a band of frequencies $\Delta\omega$ carrying the desired information, the variation of delay over this band is approximately

$$\Delta T_g \approx L \frac{d^2\beta}{d\omega^2} \Delta\omega \tag{4}$$

Thus a pulse will spread at a rate proportional to the second derivative of β with frequency. One source of such group velocity dispersion is *waveguide dispersion*, arising from the frequency dependence of β for a given guided mode, with refractive index considered independent of frequency. For step index fibers, values may be estimated from the curves plotted in Fig. 14.9*b* or calculated numerically from the implicit forms of Sec. 14.9. This contribution to dispersion is generally less important than the contributions arising from *material dispersion.*

Material dispersion arises from the variation of refractive index with frequency. From (4) with $\beta \approx \omega n/c$, this is

$$\Delta T_g \approx \frac{L}{c} \frac{d^2(n\omega)}{d\omega^2} \Delta\omega \tag{5}$$

In fiber technology it is common to express dispersion in terms of wavelength spread rather than frequency spread, with (4) written

$$\Delta T_g = LD\Delta\lambda \tag{6}$$

where D is related to $d^2\beta/d\omega^2$ by

$$D = -\frac{2\pi c}{\lambda^2} \frac{d^2\beta}{d\omega^2} \tag{7}$$

This is commonly expressed in picoseconds per kilometer of fiber length and nanometer of wavelength spread. Some representative curves of D versus wavelength[23] are shown in Fig. 14.11. Material dispersion is seen to be larger than waveguide dispersion except near the wavelength of zero dispersion, which for silica is around 1.3 μm. The zero-dispersion wavelength can be shifted by doping the material or by using multiple dielectrics in the cladding, or both. Operation near a zero-dispersion wavelength may be important in minimizing envelope distortion.

Normal dispersion ($d^2\beta/d\omega^2 > 0$ or $D < 0$) occurs for wavelengths shorter than that for zero dispersion, and anomalous dispersion ($d^2\beta/d\omega^2 < 0$ or $D > 0$) for the longer wavelengths.

For a highly coherent source such as a good laser, $\Delta\omega$ of (4) or $\Delta\lambda$ of (6) comes from the frequency spectrum of the modulated signal. For example a gaussian pulse of width τ would spread to τ' in distance L, as in Eq. 8.16(14):

$$\tau' = \tau\left[1 + \left(\frac{8L}{\tau^2} \frac{d^2\beta}{d\omega^2}\right)^2\right]^{1/2} \tag{8}$$

[23] *B. J. Ainslie and C. R. Day,* J. Light Wave Tech. ***LT-4****, 967 (1986).*

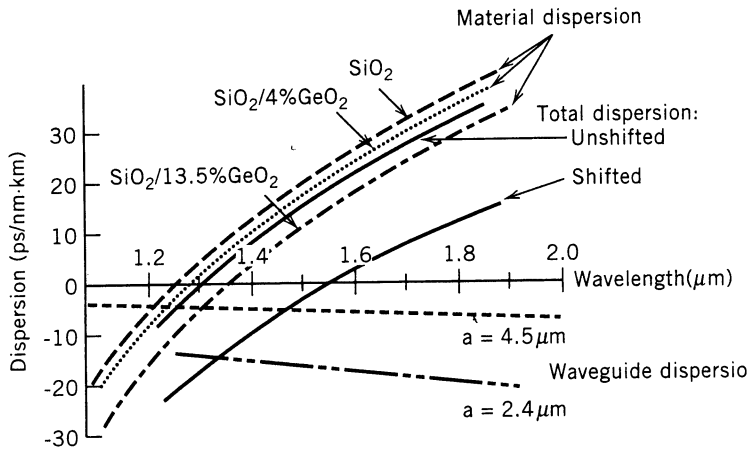

FIG. 14.11 Dispersion of single-mode fibers as function of material composition and core radius a. (After Ainslie et al.[23])

For an incoherent source such as a light-emitting diode (LED) or imperfect laser, $\Delta\omega$ or $\Delta\lambda$ may arise from the frequency variations of the source, exceeding the spectral width of the signal. In that case, the spectral width of the source is used in (4) or (6).

14.12 NONLINEAR EFFECTS IN FIBERS: SOLITONS

Silica and the related materials used in optical fibers have such a high degree of linearity that nonlinear effects might not be expected. Nevertheless, the small fiber cross sections lead to intensities high enough to produce small nonlinear interactions even with modest powers, and the low loss allows these interactions to occur over long lengths of the fiber. We shall concentrate here on the self-phase modulation effect in which refractive index changes with the intensity of the wave, which in turn changes the phase of the wave. Other important effects, some useful and some undesirable, include intermodulation products among several signals propagating in the same fiber, harmonic generation, and several parametric processes.[24] Stimulated Raman scattering arises from interaction of the optical wave with vibrational modes of the silica molecules and stimulated Brillouin scattering from interaction with acoustic waves in the fiber. Both may cause undesirable frequency shifts, but have also proven useful as optical amplifiers or tunable optical oscillators. All of these are well treated in several texts.[25]

[24] *G. P. Agrawal,* Nonlinear Fiber Optics, *Academic Press, San Diego, CA, 1989.*

[25] *See, for example, B. E. A. Saleh and M. C. Teich,* Fundamentals of Photonics, *Chap. 19, Wiley, New York, 1991; or A. Yariv,* Quantum Electronics, *3rd ed., Chap. 18, Wiley, New York, 1989.*

The important nonlinear effect in fibers, in the language of Sec. 13.7, is a $\chi^{(3)}$ effect. It is more common to express it in terms of a change in the refractive index:

$$n(E) = n_0 + \Delta n = n_0 + n_2|E|^2 \tag{1}$$

This Δn produces phase change in length L:

$$\Delta\phi = L\Delta\beta \approx \frac{L\omega}{c}\Delta n \tag{2}$$

For silica, $n_2 \approx 2.3 \times 10^{-22}$ m^2/V^2 so 10 W in a fiber of 10-μm core diameter would result in a field of about 8×10^6 V/m, producing an index change by (1) of only 1.5×10^{-8}. From (2), however, this would produce phase change of π in about 43 m for $\lambda = 1.3$ μm.

To illustrate the importance of dispersion and nonlinear index working together, we will neglect transverse variations and losses, assume small nonlinear effects, neglect dispersion terms higher than $d^2\beta/d\omega^2$, and consider only one polarization so that electric field may be treated as a scalar. Expressing the field $E(z, t)$ as a Fourier integral,

$$E(z, t) = \frac{1}{2\pi}\int_{-\infty}^{\infty} E(z, \omega)e^{j\omega t}\, d\omega \tag{3}$$

Each Fourier component propagates with its phase constant $\beta(\omega)$,

$$E(z, \omega) = E(0, \omega)e^{-j\beta z} \tag{4}$$

so that

$$\frac{\partial E(z, \omega)}{\partial z} = -j\beta E(z, \omega) \tag{5}$$

For the dispersive effect, we expand β in a Taylor series up to second-order terms, as in Sec. 8.16, and add the nonlinear perturbation. Since it is not rapidly varying with frequency, it is evaluated at ω_0:

$$\beta(\omega) = \beta(\omega_0) + \frac{\partial\beta}{\partial\omega}(\omega - \omega_0) + \frac{1}{2}\frac{\partial^2\beta}{\partial\omega^2}(\omega - \omega_0)^2 + \frac{\omega_0}{c}\Delta n \tag{6}$$

Now if we consider a pulse with envelope $A(z, t)$ modulating the optical carrier of angular frequency ω_0,

$$E(z, t) = A(z, t)e^{j(\omega_0 t - \beta_0 z)} \tag{7}$$

The pulse envelope $A(z, t)$ may be expressed in a Fourier integral in its base frequency, $\omega_m = \omega - \omega_0$:

$$A(z, t) = \frac{1}{2\pi}\int_{-\infty}^{\infty} A(z, \omega_m)e^{j\omega_m t}d\omega_m \tag{8}$$

From (7) and (8) we may show

$$E(z, \omega) = A(z, \omega_m)e^{-j\beta_0 z} \tag{9}$$

So substitution in (5) gives

$$\frac{\partial A(z,\,\omega_m)}{\partial z} - j\beta_0 A(z,\,\omega_m) = -j\beta A(z,\,\omega_m) \tag{10}$$

Now using Eq. (6) and using $d\beta/d\omega = 1/v_g$, $\beta'' = d^2\beta/d\omega^2$, and Δn from (1),

$$\frac{\partial A(z,\,\omega_m)}{\partial z} = -j\left[\frac{\omega_m}{v_g} + \frac{\beta''}{2}\omega_m^2 + \frac{\omega_0 n_2}{c}|E|^2\right]A(z,\,\omega_m) \tag{11}$$

We next make an inverse Fourier transform of (11), noting that the inverse Fourier transform of $(j\omega_m)^n A(z,\,\omega_m)$ is $\partial^n A(z,\,t)/\partial t^n$. The result is

$$\frac{\partial A(z,\,t)}{\partial z} + \frac{1}{v_g}\frac{\partial A(z,\,t)}{\partial t} = \frac{j}{2}\beta''\frac{\partial^2 A(z,\,t)}{\partial t^2} - \frac{j\omega_0}{c}n_2|A|^2 A(z,\,t) \tag{12}$$

Equation (12) is a nonlinear equation giving the effect of both dispersion and nonlinearity on wave propagation. (It is often normalized and transformed to moving coordinates, leading to a standard form known as the *nonlinear Schroedinger equation*, but the present form is adequate for our purposes.) If terms on the right were zero, the pulse amplitude $A(z,\,t)$ would travel without change at group velocity v_g as expected. The first term on the right represents group velocity dispersion and leads to pulse broadening as explained in Secs. 8.16 and 14.11. The second term on the right gives the effect of the nonlinearity, and the self phase modulation described qualitatively above.

Solitons An important solution of (12) is the fundamental soliton, or solitary wave, expressed by

$$A(z,\,t) = A_0\,\mathrm{sech}\left(\frac{t - z/v_g}{\tau_0}\right)e^{jz/4z_0} \tag{13}$$

where $z_0 = \tau_0^2/2\beta''$ and τ_0 is a measure of the width of a propagating pulse. Equation (13) is a solution for a particular amplitude satisfying the condition

$$A_0 = \frac{1}{\tau_0}\left(\frac{-\beta'' c}{\omega n_2}\right)^{1/2} \tag{14}$$

We see first that β'' must be negative for there to be a real solution of (12). That is, operation must be in the region of anomalous dispersion, which for silica occurs for wavelengths longer than about 1.3 μm. Then, for a particular amplitude related to pulse width and the characteristics of the fiber, the envelope (13) propagates at group velocity v_g without change of shape. The group velocity dispersion, which tends to make the pulse broaden, is compensated by the nonlinear effect, which tends to compress the pulse.

Although the preceding analysis has involved several idealizations, it has proven useful in predicting the observed solitons in actual fibers. Note that the true solitons exist only for specific power levels. Thus when propagating with attenuation there is

some pulse broadening as power is lost. But it is a graceful degradation, and experience has shown that additional power to restore the balance need not be added for many kilometers.

There are other solutions to (12), called higher-order solitons. These alternately broaden and contract, returning to the original shape in distance z_0.

Pulse Compression Another important application of (12) is in the compression of short optical pulses. In this technique, a fiber with normal dispersion ($\beta'' > 0$) may propagate a pulse, the nonlinear effect producing a frequency shift or "chirp" and the group velocity dispersion causing the pulse to broaden. With the right parameters, the frequency variation may be an almost linear function of time and the pulse may then be compressed by introducing separate anomalous dispersion, for example, by a combination of prisms and/or gratings. This is related to soliton propagation, except that there the anomalous dispersion is in the fiber, continuously compensating for the dispersion, and in the fiber pulse compressor the two functions are separate.

Extensive study of (12) requires numerical solution. Curves for optimum design of the pulse compressors have been so obtained.[26]

Gaussian Beams In Space and In Optical Resonators

14.13 Propagation of Gaussian Beams in a Homogeneous Medium

The modes of a graded index fiber, studied in Sec. 14.10, propagate with a constant pattern in the fiber if the modes are properly started. Any tendency to diffract is just countered by the distributed focusing effect of the lens-like medium. Let us imagine that the modes come to the end of the fiber, as in Fig. 14.13, and excite similar modes in space or other homogeneous material. It seems clear that they will spread by diffraction in the external region. Gaussian modes and their higher-order extensions thus become fundamental forms in homogeneous regions and may be excited in a variety of ways by lasers or other coherent sources. It is thus important to understand their properties.

The main propagation variation in the homogeneous region is still expected as e^{-jkz}, but there are other variations with z so that we may write

$$E(r, \phi, z) = \psi(r, \phi, z)e^{-jkz} \tag{1}$$

[26] *W. J. Tomlinson, R. H. Stolen, and C. V. Shank,* J. Opt. Soc. Am. B **1**, *139 (1984). Also see G. P. Agrawal,* Nonlinear Fiber Optics, *Chap. 6, Academic Press, San Diego, CA, 1989.*

source P located at (x_0, y_0, z_0). The idealized spherical wave (Prob. 14.19c) emanating from the source may be written as

$$A(x, y, z) = \frac{A_0}{r(x, y, z)} e^{-jkr(x,y,z)} \tag{9}$$

where

$$r(x, y, z) = [(x - x_0)^2 + (y - y_0)^2 + (z - z_0)^2]^{1/2} \tag{10}$$

After interfering with a plane reference wave of the form (6), and recording with linearity assumed as in the previous examples, transmissivity at $z = 0$ is

$$T(x, y) = K\left\{\left(\frac{A_0^2}{r^2} + R_0^2\right) + \frac{A_0 R_0}{r}\left[e^{j(\psi_0 - kr(x,y,z_0)} + e^{-j(\psi_0 - kr(x,y,z_0)}\right]\right\} \tag{11}$$

The original point source is removed and the hologram irradiated with reference wave (6), yielding a transmitted wave

$$B(x, y) = B_1 + B_2 + B_3 \tag{12}$$

where

$$B_1(x, y) = KR_0\left(\frac{A_0^2}{r^2} + R_0^2\right)\exp[-j(kz_0 + \psi)] \tag{13}$$

$$B_2(x, y) = \frac{KR_0^2 A_0}{r}\exp\{-jk[(x - x_0)^2 + (y - y_0)^2 + z_0^2]^{1/2}\} \tag{14}$$

$$B_3(x, y) = \frac{KR_0^2 A_0}{r}\exp\{-2j\psi_0 + jk[(x - x_0)^2 + (y - y_0)^2 + z_0^2]^{1/2}\} \tag{15}$$

Following previous arguments, B_2 continues to the right as a diverging spherical wave as though emanating from the original source P (now missing), and B_3 as a converging spherical wave resulting in a real image of P at P'. B_1 is uniform in phase over the plane but varying in amplitude through the dependence on r. This can be made small and the continuation of B_1 to the right is approximately a plane wave, with B_2 the desired reconstruction.

PROBLEMS

14.2a Obtain from Eq. 14.2(4) the approximate spread of focal length Δf from $r = 0$ to r_{max} when $r_{max}/R \ll 1$. For a spherical mirror of radius of curvature 1 m, used with a laser of wavelength $\lambda_0 = 1$ μm, give the maximum radius of rays from the axis if spread in focal length is not to be more than a wavelength.

14.2b The f-number of a lens is defined as the ratio of focal length to diameter. (Here we will denote by F to avoid confusion with focal length.) Give the spread of focal

length in terms of F when $r_{max} \ll R$ for the spherical mirror. Explain why "stopping down" a lens to higher values of F should increase sharpness of an image.

14.2c Carry out the derivation corresponding to that of Ex. 14.2c for a diverging thin lens with plane surface at $z = 0$ and a parabolic surface $z = d + r^2/4g$, $0 < r < a$, (i) by ray analysis and (ii) by phase considerations.

14.2d For the doubly convex lens of Fig. 14.2*e*, derive the equation for focal length, Eq. 14.2 (21), by considering refraction at the surface.

14.2e Consider the imaging for a spherical mirror by ray reflection. That is, for an object point on the axis distance d_1 from a mirror with radius of curvature R, find the image distance d_2 from the mirror at which a ray reflected at radius r crosses the axis. Under what approximations does Eq. 14.2(24) apply?

14.3a For a uniform plane wave, polarized with e_z only, propagating at angle α from the x axis with $\cos\gamma = 0$, give all quantities $\mathbf{e}$, $\mathbf{h}$, S, u_e, and u_h used in the general formulation. Material has refractive index n.

14.3b We will find later that many useful beams have gaussian forms. Assume one with form in the transverse plane, $\mathbf{e} = \hat{\mathbf{x}} \exp[-(x^2 + y^2)/w_0^2]$ propagating substantially in the z direction, $S \approx nz$. Compare the neglected term on the right side of Eq. 14.3(5) with the term $\nabla S \times \mathbf{e}$ in magnitude and direction and state under what condition it is negligible.

14.3c Utilizing Eq. 14.3(12) for the eikonal of a plane wave, show that $\mathbf{E}$ and $\mathbf{H}$ are related as in an arbitrarily propagating plane wave in a homogeneous medium.

14.4a Find the required form of refractive index variation to maintain a ray in a circular path of constant radius R.

14.4b Very low absorptions can be measured by using the thermal lens effect resulting from passing a beam through a cell containing the sample, as in Ex. 14.4a. It has been shown [J. R. Whinnery, *Acc. Chem. Res.* **7**, 225 (1974)] that the heating effect results, in steady state, in a quadratic index variation near the axis as in Eq. 14.4(11), with

$$\Delta = -\frac{\alpha P(dn/dT)}{4\pi k n_0}$$

where α is absorption coefficient, P power in the laser beam, dn/dT the variation of refractive index with temperature, k the thermal conductivity, and n_0 the refractive index on the axis. Find the expected focal length of a cell 1 cm long filled with carbon disulfide ($n_0 = 1.63$, $dn/dT = 7.9 \times 10^{-4}\,\mathrm{K}^{-1}$, $k = 6.82 \times 10^{-4}$ J/cm-s-K, $\alpha = 6 \times 10^{-4}\,\mathrm{cm}^{-1}$) for a laser beam with 0.5 W power and a beam radius $a = 0.5$ mm.

14.4c Derive Eq. 14.4(4) from Eq. 14.4(10).

14.4d A typical graded index fiber used in an optical communications system with moderate data rates has $n_0 = 1.5$, $\Delta = 0.005$, and $a = 25\ \mu$m. For a ray crossing the axis at an angle r_0' find the distance at which it returns to the axis. What is the maximum angle of crossing to maintain r_{max} less than a?

14.5a A ray passes from a medium of index n_1 into a slab of thickness d and index n_2, then exits into n_1. Compare radius and slope at the output from the ray matrix and an exact Snell's law calculation if $n_1 = 1$, $n_2 = 2$, $d = 1$ cm, and angle of input ray is (i) 20 degrees and (ii) 40 degrees from the perpendicular to the slab.

14.5b Slabs of dielectric with index n_1 and thickness d_1 alternate with slabs having index n_2 and thickness d_2. Using the paraxial (small-angle) approximation, find the ray matrix for one period of this combination, then two periods, and induce the result for N periods. Interpret the result.

14.5c Derive Eq. 14.5(5) with the approximations stated.

14.5d For the doubly convex lens of Fig. 14.2*e*, derive the expression for focal length, Eq. 14.2(21), by considering the tandem combination of two spherical dielectric interfaces, with proper attention to sign.

14.6a An alternate form of the solution in Eq. 14.6(7) to the difference equation for the periodic lens system is

$$r_m = C_1 \cos m\theta + C_2 \sin m\theta$$

Relate C_1 and C_2 to the values of initial radius and slope of the rays. The ray matrix for one period is assumed known.

14.6b A periodic lens system has $d_1 = d_2$ and $f_1 = f_2 = d_1/5$. Check stability and sketch the ray paths through a few lenses starting with zero slope and $r = 0.1f_1$ at the first lens.

14.6c Repeat Prob. 14.6b for $d_1 = d_2$, $f_1 = f_2 = d_1$.

14.6d Repeat Prob. 14.6b for the case of alternate converging and diverging lenses, $d_1 = d_2$, $f_1 = -f_2 = d_1$.

14.7a Explain why sinusoidal rather than hyperbolic solutions are required in the film of Fig. 14.7*a* for guided modes with exponential decay away from the film in cover and substrate regions.

14.7b In the example of the glass film guide given in Sec. 14.7, thickness d is increased to 2 μm. Use Fig. 14.7*b* to find n_{eff} for all of the guided TE and TM modes.

14.7c In a certain semiconductor laser, the active region consists of a layer of GaAs 0.3 μm thick, with $n_2 = 3.35$. This is surrounded above and below with GaAlAs with $n_1 = n_3 = 3.23$. Use Fig. 14.7*b* to find the modes that can be guided by this active layer, and their values of n_{eff}. Wavelength λ_0 is 0.85 μm.

14.7d* To illustrate the graphical method of solution for Eq. 14.7(7), consider the symmetric case with $n_1 = n_3$ so that $q = p$. Show that (5) is then satisfied either by $pd = hd \tan(hd/2)$ or $pd = -hd \cot(hd/2)$. Sketch some curves of pd versus hd from these equations. Then show from (4) that the loci for constant v [defined by (6)] in the pd versus hd plane are circles and sketch these for $v = 2, 5, 8$. Solutions (modes) are given by points of intersection between the circles and the first sets of curves plotted. (Note that p must be positive for guided modes.) Check the modes predicted for the three values of v from Fig. 14.7*b*.

14.7e* Find the approximation to Eq. 14.7(7) when $n_3 - n_1 \gg n_2 - n_3$, as is the case for many guides with dielectric substrates but air above. Show that a graphical solution similar to that of Prob. 14.7d may be utilized for this case also.

14.8a A guide is fabricated as in Fig. 14.8*a* with the guiding material GaAs with $n_1 = 3.59$, width 1.8 μm, and depth 0.3 μm. The surrounding material is AlGaAs with $n_3 = 3.385$ except for the top surface, which is protected by silica with $n_2 = 1.5$. Free-space wavelength is 0.85 μm. Find approximate values of n_{eff} for this guide by the effective index method, for the lowest-order mode.

14.8b We are to design a dielectric guide by in-diffusing titanium into lithium niobate, much as in Fig. 14.8*b*. Assume index change Δn and diffusion depth d as in H. Naitoh *et al.*, *Appl. Opt.* **16**, 2546 (1977): $\Delta n = 0.078t^{-0.85}$ and $d = 0.43t$, where t is diffusion time in hours and d is in μm.

(i) As a first approximation, use the model of a step index guide as in Fig. 14.7*a* with air above and estimate the maximum diffusion time for single-mode operation. Take $\lambda = 0.633$ μm and the refractive index of lithium niobate as 2.05.

(ii) For operation with a v value 0.75 of that above, give diffusion time and effective index as based on this model.

(iii) Now, taking into account lateral confinement with a width 1.5 μm, use effective index method to give the next correction to n_{eff}.

14.9a For a step index fiber of silica ($n = 1.500$) cladding on a glass ($n = 1.505$) core of 6.0-μm diameter, find the cutoff wavelengths of the two lowest axially symmetric TE modes.

14.9b A fiber with $a = 10$ μm has $n_1 = 1.51$ and $n_2 = 1.50$. Use Fig. 14.9*d* to estimate the number of modes that may propagate at $\lambda_0 = 1.3$ μm. Give the values of n_{eff} for the highest and lowest order of these modes. What radius would be required for only one propagating mode?

14.10a For a fiber with quadratic index variation having $n(0) = 1.5$, $a = 10$ μm, and $\lambda_0 = 1$ μm, what Δ is required for a beam radius $w = 3$ μm? Find the percentage difference of phase velocity from that of a plane wave in material with index $n(0)$ for a fundamental mode and Hermite–gaussian modes of order m, p.

14.10b For the numerical values given in Prob. 14.10a, estimate the term on the right of Eq. 14.10(6) in comparison with the second term on the left.

14.10c Using Eq. 14.10(17) show that (16) does satisfy (15) with the conditions on w and β_{mp} as given.

14.10d* Using Eq. 14.10(23) show that (22) satisfies (21) with the conditions on w and β_{mp} as given.

14.11a A multimode fiber has $n_1 = 1.51$ and $n_2 = 1.50$. About what maximum data rate could be used with this fiber over a distance of 7 km?

14.11b If one uses the expression 14.10(19) rather than the approximation (20), group velocity does depend upon mode order. Find group velocity from (19) and the intermode dispersion based upon this result. (In a practical case, the boundary effect at $r = a$ and the departure from the ideal profile may be more important, but this is at least one component of dispersion.)

14.11c For a GaAlAs laser source at $\lambda_0 = 0.85$ μm with a single-mode fiber, material dispersion is likely to be dominant. If $d^2n/d\lambda^2 \approx 3.2 \times 10^{10}$ m^{-2} at this wavelength, what approximate data rate is usable over a length of 20 km if the laser is (i) an ideal coherent source? (ii) Has a spectral width $\Delta\lambda_0 = 0.2$ nm?

14.11d The wavelength of minimum attenuation for silica is about 1.55 μm. Use Fig. 14.11 to estimate the usable distance for a data rate of 1 Gb/s, using an unshifted fiber at this wavelength assuming perfectly coherent sources.

14.11e Under what conditions does Eq. 14.11(8) reduce to the simpler Eq. 14.11(4)? For $\tau = 10$ ps and $\lambda = 1.5$ μm, how small must the $\Delta\lambda$ of the laser be for the signal spectrum to be dominant over the source spectrum?

14.12a Show that Eq. 14.12(13) is a solution of (12) for the conditions stated.

14.12b For a silica fiber of core diameter 10 μm and refractive index 1.5, estimate the power required to maintain a fundamental soliton if wavelength is 1.4 μm with dispersion estimated as 5 ps/nm-km.

14.13a Verify the form in Eq. 14.13(12).

14.13b A typical helium–neon laser with $\lambda_0 = 633$ nm has a beam radius of about 0.5 mm. Taking this as w_0, find beam radius at the other side of a bay 10 km away. Similarly find beam radius on the moon of a Nd–YAG laser ($\lambda_0 = 1.06$ μm) 3.84×10^3 km from the earth where it starts with $w_0 = 5$ mm.

14.13c For the examples of Prob. 14.13b, there is an optimum w_0 to produce minimum beam radius at the receiver a given distance away. Find the optimum w_0 and the corresponding $w(z)$ at the targets, for the two examples of that problem.

14.13d** Show that Eq. 14.13(18) is a solution of (2) in rectangular coordinates.

14.13e** Show that Eq. 14.13(19) is a solution of (2) in circular cylindrical coordinates.

14.13f* Note that in contrast to the gaussian beam, a beam with Bessel function variation in radius,

$$E = E_0 J_0(\alpha r) e^{j(\omega t - \beta z)}$$

does not vary as it propagates in z and has been proposed for some applications [J. Durnin, *J. Opt. Soc. Am.* **A4**, 651, (1987)]. Show under what conditions it is a solution of the wave equation. Find the power propagating in an annular ring between the zeros m and $m + 1$ of the Bessel function and show that this is independent of m for large m. Discuss the advantages and disadvantages of the profile as compared with the gaussian.

14.14a A gaussian beam of beam radius w_1 and radius of curvature R_1 passes from dielectric with index n_1 to one with index n_2, the plane interface being normal to the beam axis. Find gaussian beam properties in medium 2.

14.14b One practical problem is that of focusing the output of a laser, assumed to be of fundamental gaussian beam form, onto a fiber distance L away. If beam radius of the laser (assumed a waist) is w_1 and that at the fiber (also a waist) is w_2, find position d from the laser and focal length f of a thin lens for the desired focusing. (*Hint:* Work forward from the laser and backward from the fiber until gaussian beams intersect.)

14.14c This is a variation of Prob. 14.14b in which there is a specific lens with given focal length f, but its placing and the laser-fiber spacing L are variable. Find d and L for the given w_1, w_2, and f in this case.

14.14d In the rod with quadratic index variation described in Sec. 14.10 [$n(0) = 1.5$, $\Delta = 0.01$, $\lambda_0 = 1$ μm, $a = 50$ μm], a gaussian beam is introduced with zero slope but $w(0) = 12$ μm. Describe the beam propagation for $z > 0$.

14.14e This is similar to Prob. 14.14d except that the gaussian beam is introduced into the graded index fiber at the equilibrium radius but with slope $dw/dz = 0.2$.

14.15a Derive Eq. 14.15(8) from Eqs. (5), (6), and (7).

14.15b For a helium–neon laser, the discharge tube has a diameter of 5 mm and length of 40 cm. A plane mirror is placed at one end and it is desired to keep gaussian beam diameter not more than 3 mm at the other end to minimize wall losses. Find the

radius of curvature of a mirror to be placed close to the second end. Wavelength is 633 nm. Comment on the two solutions.

14.15c For a typical solid-state laser such as ruby, Nd–YAG, or alexandrite, $a_1 = a_2 \approx$ 5 mm, $d \approx 10$ cm, and $\lambda_0 \approx 1$ μm with refractive index ≈ 1.7. Check the condition on Fresnel number N for stability of such resonators. (Note that dielectric discontinuity at the crystal side boundary further confines the beam.)

14.15d The resonator for a CO_2 laser with $\lambda_0 = 10.6$ μm has radii of curvature $R_1 =$ 10 m, $R_2 = 20$ m (sign convention as in Fig. 14.14*a*) and spacing $d = 1.5$ m. Show location on the stability diagram in Fig. 14.6*c* and find radius and position of the beam waist and the beam radii at the two mirrors.

14.15e A half-confocal resonator is made by inserting a plane mirror at the midplane of a symmetric confocal resonator. The resulting resonator has $R_1 = 2d$, $R_2 = \infty$, and by an image argument, would seem to be equivalent to the original symmetric resonator. Check the *ABCD* matrix for a round trip of this resonator and comment on the differences from the symmetric confocal resonator.

14.16a Show location on a stability diagram of the resonators of Probs. 14.15b and d and of the half-confocal resonator of Prob. 14.15e.

14.16b A ruby rod 10 cm long has refractive index $n = 1.77$ at free-space wavelength $\lambda_0 = 0.6943$ μm. If the plane ends form the resonant reflectors, find the longitudinal mode number l nearest to the given wavelength and the frequency separation between longitudinal modes.

14.16c The ruby rod of Prob. 14.16b now has its ends ground to form a confocal resonator. Give the radius of curvature needed and calculate minimum spot size and spot size at the ends. For a given mode number l, how much is frequency shifted from the value for the plane mirrors?

14.16d Find longitudinal mode separation and transverse mode separation for the resonators of Probs. 14.15b and d.

14.16e Show that there are stable configurations in which the mirror curvatures are in the same direction. That is, the mode exists between a concave and convex surface.

14.17a Supply the details of the derivation of Eq. 14.17(9) with the definitions noted in the text.

14.17b Show specifically by use of Eq. 14.17(9) that a gaussian beam at the input focal plane does transform to a gaussian at the output focal plane, as stated in the text.

14.17c Convert the integral of Eq. 14.17(6) to polar coordinates (r, ϕ) and find the form of ψ at the output focal plane if that at the input focal plane corresponds to a uniformly illuminated circle of radius a, centered on the axis.

14.18a By using two successive Fourier transforms of form Eq. 14.17(6), show that when $T_2(x_2) = 1$, the $\psi_3(x_3)$ of Fig. 14.18*b* is like the input function but inverted and changed in scale.

14.18b In Ex. 14.18 suppose that the spatial filter passes only lines $\pm n$ but with a π-phase shift for $-n$ and zero-phase shift for $+n$. Describe the output function $\psi_3(x_3)$.

14.18c Extend Ex. 14.18 to a two-dimensional screen with both horizontal and vertical gratings. Describe the pattern for the Fourier plane. Design a spatial filter so that only a horizontal grating appears at plane 3.

14.19a In holography the reference wave need not be a plane wave. Consider Ex. 14.19a with the object wave a plane wave incident at an angle on the recording plane and the reference a spherical wave:

$$R(x, y, z) = R_0 \exp\{-jk[x^2 + y^2 + (z - z_1)^2]^{1/2}\}$$

Find $T(x, y)$ in the plane $z = 0$ and the transmitted wave when the resulting hologram is irradiated with this R.

14.19b As in Prob. 14.19a but with the object wave a spherical wave as in Ex. 14.19b.

14.19c It was shown in Chapter 12 that a spherically symmetric wave of the form 14.19(9) is not a solution of Maxwell's equations. Discuss the concept of a point source in optics and the conditions under which (9) may be a useful approximation.

14.19d A hologram may be made of the Fourier transform of a two-dimensional function by combining concepts of this section and the preceding two. Sketch an arrangement for making such a Fourier transform hologram.